

Extrinsic Fabry–Perot Interferometer for Measuring the Stiffness of Ciliary Bundles on Hair Cells

Matthew D. Barrett, Ellengene H. Peterson, and J. Wallace Grant*

Abstract—We have developed an extrinsic Fabry–Perot interferometer (EFPI) to measure displacements of microscopic, living organelles in the inner ear. The EFPI is an optical phase-shifted instrument that can be used to measure nanometer displacements. The instrument transmits a coherent light signal to the end of a single glass optical fiber where the measurement is made. As the coherent light reaches the end of the fiber, part of this incident signal is reflected off the internal face of the fiber end (reference reflection) and part is transmitted through the end of the fiber. This transmitted light travels a short distance and is reflected off the surface whose displacement is to be measured (the target). This sensing reflection then reenters the fiber where it interferes with the reference reflection. The resulting interference signal then travels up the same optical fiber to a detector, where it is converted into a voltage that can be read from an oscilloscope. When the target moves, the phase relation between reference and sensing reflections changes, and the detector receives a modulated signal proportional to the target movement. Reflections of as little as 1% at both the sensor tip and target surfaces produce good results with this system.

We use the EFPI in conjunction with fine glass whiskers to measure the stiffness (force per unit deflection) of stereociliary bundles on hair cells of the inner ear. The forces generated are in the tenths of picoNewton range and the displacements are tens of nanometers. Here we describe the EFPI and its development as a method for measuring displacements of microscopic organelles in a fluid medium. We also report experiments to validate the accuracy of the EFPI output and preliminary measurements of ciliary bundle stiffness in the posterior semicircular canal.

Index Terms—Biomechanics, fiberoptics, hair cells, interferometry, stereocilia, submicron displacements.

I. INTRODUCTION

THE GOAL of this work is to develop a more accurate method for measuring the stiffness of ciliary bundles on hair cells. Hair cells are mechanoreceptors that vertebrates use to detect sound, water- or substrate-borne vibrations, head accelerations, and the equivalent acceleration of gravity. The mechanoreceptive element of a hair cell is its ciliary bundle, a collection of hair-like processes that extend from the apical surface of the hair cell and are deflected by force-generating

Manuscript received June 12, 1997; revised July 22, 1998. This work was supported by the National Science Foundation (NSF) under Grant IBN-9319630. Asterisk indicates corresponding author.

M. D. Barrett is with the Biomechanics Engineering Program, Department of Engineering Science and Mechanics, Virginia Polytechnic Institute and State University, Blacksburg, VA 24060-0219 USA.

E. H. Peterson is with the Department of Biological Sciences and Neurobiology Program, Ohio University, Athens, OH 45701-2979 USA.

*J. W. Grant is with the Biomechanics Engineering Program, Department of Engineering Science and Mechanics, Virginia Polytechnic Institute and State University, Blacksburg, VA 24060-0219 USA (e-mail: jgrant@vt.edu).

Publisher Item Identifier S 0018-9294(99)01849-2.

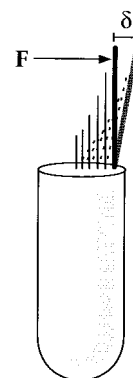


Fig. 1. Schematic representation of a vertebrate hair cell with a ciliary bundle extending from its apical surface (solid lines). The hair cell generates a signal when a force (F ; e.g., movement of the gel layer in which the bundle is imbedded) deflects the ciliary bundle. The magnitude of the signal is a function of deflection magnitude (δ), and δ , in turn, depends on F and on bundle stiffness (k). In experiments to measure the stiffness, the force step (F) is applied to the tip of the bundle; for living vestibular bundles this is the tip of the kinocilium (thick black line).

elements in the lateral line canals or inner ear (e.g., cupula, otolithic membrane) (Fig. 1).

A ciliary bundle's response to mechanical stimuli is determined by its stiffness, k

$$k = F/\delta \quad (1)$$

where F is the force applied to the bundle and δ is the resulting deflection (Fig. 1). Thus, it is important to know the stiffness of a ciliary bundle if we are to understand how it detects and encodes mechanical stimuli. But measuring the stiffness of ciliary bundles presents several challenges. First, ciliary bundles are microscopic, living organelles. Thus, they must be visualized with specialized optics and maintained in a suitable fluid medium if measured stiffnesses are to reflect the normal, living state. Second, the forces that a bundle must transduce are in the picoNewton range, and physiologic displacements are typically much less than 500 nm. Thus, accurate stiffness determinations require precise measurements of very small forces and displacements. Finally, bundles should be assessed *in situ*, i.e., while the parent hair cell retains its normal position in the sensory epithelium. This minimizes mechanical disruption of delicate bundle components and preserves information about the hair cell's normal epithelial location, which can provide important clues about the hair cell's identity and function.

Previous studies of bundle stiffness have met these challenges in several ways. Investigators have measured bundle

stiffness on *in situ* [1]–[5] or dissociated [6], [7] hair cells, or on epithelia that have been digested and stripped from their connective tissue base [8]. They have measured displacements with optical techniques such as light microscopy [5], magnified digital images [7] or photodiode pairs [1]–[4], [6], [7], and with interferometry [8]. They have applied forces to bundles with fine probes advanced via a piezo stepper [1]–[4] and with water jets [6], [7], [9], [10], or they have relied on Brownian motion [8]. Each of these options has advantages and disadvantages, but in no case have preparation, measurement, and displacement methods been combined for optimal accuracy in characterizing bundle stiffness and stiffness differences between different hair bundle types. Our approach has been to combine the advantages of *in situ* measurement with the superior precision of interferometry. We use the interferometer to measure both the stimulus to the bundle and the bundle's response, which further increases the accuracy of our stiffness calculations.

This work relies on new instrumentation: a two-channel sensor that utilizes laser interferometry and an optical fiber delivery system. The sensor is a low-finesse (low mirror reflectivity) Extrinsic Fabry–Perot interferometer (EFPI): a quadrature phase-shifted, optical fiber sensor that uses an extrinsic Fabry–Perot cavity for the measurement [11]. Each channel of the instrumentation is actually a separate interferometer where the two channels use a single laser source for monochromatic light. All other elements of a channel are duplicated. One channel of the EFPI measures the displacement step delivered to the bundle; the second channel measures the bundle's deflection. In this paper, we describe our protocol for measuring ciliary bundle stiffness and the new instrument.

II. EQUIPMENT AND METHODS

A. Experimental Protocol

Fig. 2 illustrates the procedure we use to measure bundle stiffness. We deflect the ciliary bundle using a glass whisker of known stiffness (see Glass whisker manufacture and calibration, below). This displacement whisker is glued to a glass pipette, which is attached to a piezo stepper (Nanostepper; WPI). We position the tip of the displacement whisker against the tip of the ciliary bundle [Fig. 2(a)] and step the pipette/whisker base by a distance Δx_P [from position A to position B in Fig. 2(b)]. The bundle displaces by distance Δx_B , and the whisker deflection Δx_W is

$$\Delta x_W = \Delta x_P - \Delta x_B \quad (2)$$

[Fig. 2(b)]. We measure Δx_P with one channel of the EFPI and Δx_B with the other channel.

Bundle stiffness can be calculated from these two displacement measurements if the glass whisker's stiffness is known. Using the relation between force, displacement, and stiffness (1) and the fact that—for these steady state experiments—contact forces between the whisker and the bundle are equal and opposite, we have

$$k_B \Delta x_B = k_W \Delta x_W. \quad (3)$$

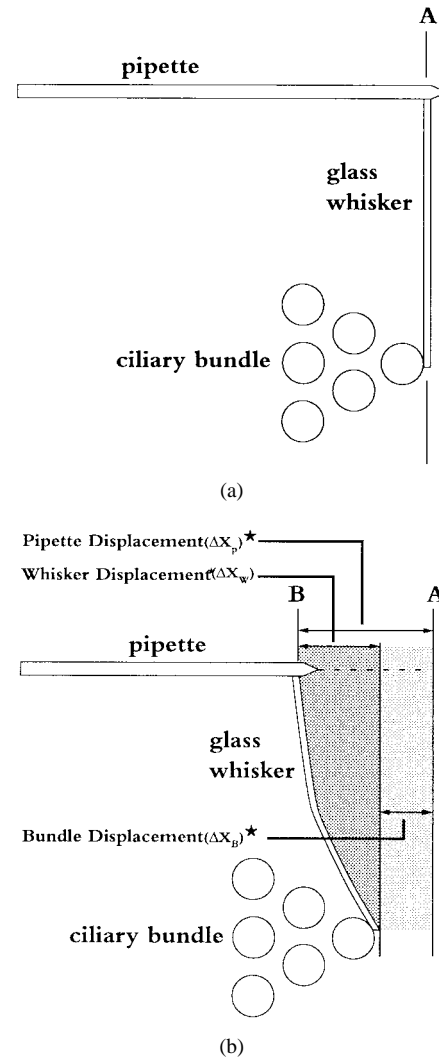


Fig. 2. Procedure for measuring ciliary bundle stiffness. The pipette-whisker-bundle complex is shown as it appears during an experiment and is viewed from above: (a) start position. The whisker tip is positioned against the tip of the kinocilium (position A) and (b) final position. The pipette is displaced from position A to position B (Δx_P) using a piezo stepper. We set the piezo device to move $<1 \mu\text{m}$, and we measure the actual movement with our EFPI. We deflect the ciliary bundle using a glass whisker of known stiffness (K_W) adhesively bonded to a pipette. The resulting bundle displacement (Δx_B) depends on the stiffness of the glass whisker (K_W) and the stiffness of the bundle (K_B). We manufacture the displacement whisker to be more compliant than the bundle. Thus, bundle-whisker tip displacement is always $<$ pipette base, i.e., $<325 \text{ nm}$ [see Fig. 4(b), top; Fig. 6].

Substituting for Δx_W (2) and solving for bundle stiffness gives

$$k_B = k_W \left(\frac{\Delta x_P}{\Delta x_B} - 1 \right). \quad (4)$$

This stiffness measurement protocol has two advantages. First, we measure bundle displacement and the step applied to the bundle. This is probably more accurate than relying on the stated output of the piezo stepper, which we found to be unreliable. Second, we use a ratio of displacements to calculate bundle stiffness (4), which removes any constant error in Δx measurements. In control experiments (28 trials) we demonstrated that the two EFPI channels give nearly identical displacement values (3% error) when recording movement of the same object. Thus, differences between Δx_P and Δx_B

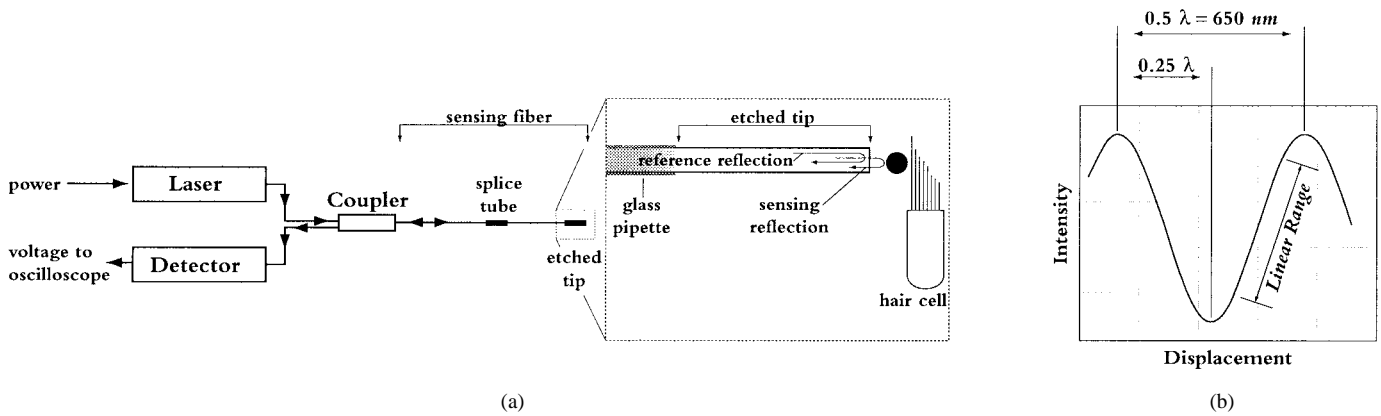


Fig. 3. EFPI for measuring ciliary bundle stiffness: (a) light from a 1300-nm laser is transmitted to the epithelium over an optical fiber. The end of the fiber is mounted in a glass pipette (inset), which can be positioned by a micromanipulator. The free tip of the fiber is etched to reduce its diameter. We position the etched tip so that it is normal to the displacement whisker (Inset: black circle) and the bundle. Light traveling down the tip is reflected from the end of the optical fiber (reference reflection) and from the displacement whisker (sensing reflection) back into the optical fiber. The resulting interference between reference and sensing reflections is read by the detector and converted to an output signal (voltage) that is proportional to displacement and (b) schematic output of EFPI showing cosinusoidal relation between output voltage and displacement. One full cycle of the voltage indicates a displacement of 650 nm ($1/2\lambda$; λ = wavelength). To measure displacements of more than 325 nm—such as the base of the pipette during a stiffness measurement (Δx_P)—we count voltage cycles [Fig. 4(b), bottom] To measure the small (<325 nm) displacements that ciliary bundles experience during normal behavior we select a starting gap distance such that the output voltage remains within its (approximately) linear range during the stiffness measurement [Fig. 4(b), top; Fig. 6].

reflect real differences between the displacement stimulus Δx_P and the bundle's response Δx_B . The 3% error between measurements of the same movement means that stiffness differences between bundles must be greater than 3% to be discriminable by our current system.

B. Displacement Whisker Manufacture and Stiffness Determination

We manufacture displacement whiskers from borosilicate glass rods pulled to a tip diameter of 2–4 μm with a micropipette puller (Flaming-Brown, Sutter Instrument Co., San Rafael, CA). Then we pull the whiskers to a final length of 200–400 μm and a diameter of 1–2 μm using a microforge (Stoelting Co., Wood Dale, IL). We adhesively bonded these displacement whiskers to micropipettes (1- to 2-mm long, 10- to 25- μm diameter) at a 90° angle (Fig. 2).

The stiffness of our displacement whiskers was calculated by attaching 30- to 100- μm diameter para-methyl-styrene spherical beads of known density ($\rho = 1.030 \text{ g/cm}^3$; Bangs Laboratories, Inc., Carmel, IN) to the whisker electrostatically, and measuring the resulting whisker displacement. We view the whisker and attached bead with the microforge optics and measure bead diameter and whisker deflection with an eyepiece reticule. We calculate the weight of the bead from its diameter and density and use this weight to determine the displacement whisker's stiffness. We also measure the distance from the whisker base to the point of bead attachment (because beads do not always attach to the whisker tip) and corrected our whisker stiffness calculations accordingly. We use a minimum four to six beads of different sizes to assess each whisker, and the average stiffness is used as the whisker stiffness (k_W).

C. Extrinsic Fabry–Perot Interferometer (EFPI)

Optical interferometers that use a coherent light source are useful devices for measuring small displacements accurately.

They use two signals that can vary in path length and, consequently, in phase; any phase difference between the two signals results in constructive and destructive interference, which modulates the intensity of the output. Displacements create such a phase difference between the two optical signals; thus, they can be measured using interferometry. Because displacements are assessed relative to the wavelength of light, which is very small, displacement measurements via optical interferometry have extremely high resolution.

For this work we used an optical fiber Fabry–Perot interferometer. This multiple beam device detects the interference of signals reflected from two parallel surfaces that are separated by a small gap. In an *intrinsic* Fabry–Perot interferometer, the two reflecting surfaces are the facing ends of a cleaved fiber that are aligned within a chamber (the Fabry–Perot cavity) and separated by a gap distance; environmental disturbances (e.g., temperature fluctuations) modulate this gap distance and thus the signal at the detector [12]. In an *extrinsic* Fabry–Perot interferometer, the two reflecting surfaces are the air–fiber interface at the cleaved end of the optical fiber and the interface at the far end of the air gap [11]. We chose an EFPI for this work because of the superior resolution of multiple beam interferometers [13], because its output is a linear function of axial displacement over the range of small displacements we wish to measure [14], and because the small sensor tip can be positioned under the objective of a light microscope to record displacements of living organelles.

1) *Equipment Description:* The EFPI consists of five components [Fig. 3(a)]. 1) A *laser diode* provides the coherent light source. A single diode provides light for each channel of the instrument, other components are duplicated to create two separate channels for measurement. 2) The *coupler* is a bidirectional splicing device that transmits light from the laser diode to the sensing fiber and the return signal from the sensing fiber to the detector. 3) A *sensing fiber* transmits light bidirectionally between the coupler and the sensor tip. This

sensing fiber is interrupted by a *splice tube*, which allows the delicate sensor heads to be easily replaced. 4) The *sensor tip* is positioned normal to the reflective surface whose displacement is to be measured [Fig. 3(a), inset]. The tip can be etched with hydrofluoric acid to remove its fiber cladding and reduce the sensor's diameter if this is required by the experiment. In this experiment we etched the tip to about 33- μm diameter. The space between the sensor tip and the target is the extrinsic Fabry-Perot cavity. 5) A detector, comprising a photodiode transducer and associated electronics, converts the interference signal into a voltage that can be displayed on an oscilloscope. The detector's voltage output is a linear function of the interference intensity. The EFPI was fabricated by the Fiber & Electro-Optics Research Center at Virginia Polytechnic Institute and State University, Blacksburg, VA; they also verified the linear relationship between the interference signal and the voltage output.

2) *Operation*: A monochromatic, coherent light ($\lambda = 1300$ nm, i.e., infrared) travels down the sensing fiber [Fig. 3(a)]. At the sensor tip, part of the light is reflected at the interface between the fiber tip and the external air or fluid medium [*reference reflection*; Fig. 3(a), inset]. The remaining light travels through this interface and is reflected by the target (*sensing reflection*). In the present context, the target is the deflection whisker (black circle), which is in contact with the ciliary bundle. The sensing reflection re-enters the sensing fiber and interferes constructively and destructively with the reference reflection. Any movement of the deflection whisker and resulting modulation of the return signal intensity is read by the detector and converted to an output voltage. Reflections of as little as 1% at both the reference and reflection surfaces produce good results with the system.

For a low-finesse EFPI (reflections as low as 1%), the intensity of the reference and sensing signals can be represented mathematically by a plane wave approximation in which the complex amplitude A_1 is the reference signal and A_2 is the sensing signal. The intensity of the returning signal at the detector I_{det} can be expressed as a superposition of the two amplitudes

$$I_{det} = A_1^2 + A_2^2 + 2A_1A_2 \cos(\phi_1 - \phi_2) \quad (5)$$

where ϕ_1 is the phase of the reference reflection and ϕ_2 is the phase of the sensing reflection. Thus, the signal that returns to the detector has a constant component and a component that varies as the cosine of the phase shift between the reference and sensing reflections.

The EFPI response to a target displacement is expressed as a cosinusoidal oscillating voltage that reflects the phase shift (change in path length) between sensing and reference reflections [Fig. 3(b)]. The change in path length is twice the distance that the target moves because the sensing reflection must cross the air or fluid gap twice: as outbound and return signal. Accordingly, a 360° phase angle cycle represents a target displacement of 0.5λ or 650 nm; a 180° phase cycle (e.g., the peak-to-peak intensity) represents a 0.25λ or 325-nm displacement.

3) *Calibration*: The intensity of the return signal at the detector depends on the gap distance between the sensor tip

and the target [14] and on the amplitude of the reference and sensing signals [A_1 and A_2 in (5)]. A_1 and A_2 vary with the idiosyncratic reflectances of the sensor tip and the target, respectively. Thus, the signal that arrives at the detector must be calibrated for each experiment, i.e., for the specific sensor tip and target (deflection whisker) and for their starting (gap) distance relative to each other.

Calibration requires relative movement between the sensor tip and target sufficient to yield a peak-to-peak intensity change. In practice, the calibration step is greater than 650 nm; thus it yields at least one 360° intensity cycle. Either the sensor tip or the target can be moved. As noted above, their displacement relative to each other produces a sinusoidally oscillating voltage in which the peak-to-peak voltage represents 325 nm of movement [Fig. 3(b)].

To measure displacements of less than 325-nm, calibration must precede the measurement. Once the peak-to-peak voltage for a 325-nm displacement is determined by calibration, smaller displacements can be inferred by linear interpolation. In such cases, it is desirable to position the sensor tip and target (i.e., set the gap distance) such that the trace starts near the beginning of the approximately linear region of the output signal; thus output voltages can be linearly related to displacement [Fig. 3(b)]. We chose the wavelength of laser ($\lambda = 1300$ nm) with this in mind. The linear range of the output signal corresponds to approximately 300 nm (this is the portion of the sine curve that is approximately linear), which is larger than the bundle displacements we wish to measure. Thus, the signal from the bundle can be encompassed within the linear range of the output. For displacements greater than 325 nm, a calibration (peak-to-peak) intensity can be extracted from the measurement itself. One simply counts intensity cycles and adds the remaining fractional cycle to determine total displacement. We used this method to measure the step applied to the displacement whisker (i.e., the stimulus to the bundle).

4) *Minimum Detectable Displacement (MDD)*: There is some noise in the output (voltage signal) of the EFPI. This noise originates from thermal instabilities in the system circuitry, photodiode detector, the laser-diode light source, and even potentially from mechanical vibration (the measurements were made on a vibration isolation table to eliminate mechanical noise). So the system output noise is a sum of all these potential sources. No singular source could be identified as a major contributor to the total system noise.

This noise determines the minimum displacement that our current system can detect. To assess this MDD, we first determine the signal-to-noise ratio (SNR)

$$\text{SNR} = \frac{\Delta V_{\text{signal}}}{\Delta V_{\text{noise}}} \quad (6)$$

where ΔV_{noise} is the peak-to-peak voltage in the unstimulated system, and ΔV_{signal} is the peak-to-peak voltage during calibration. (Note: voltages here are proportional to optical powers and the SNR is optical power based.) Both are read from the storage oscilloscope monitoring the output (LeCroi 9410 Dual

150-MHz Digital Oscilloscope). The MDD is

$$\text{MDD} = \frac{\lambda}{4} \left(\frac{1}{\text{SNR}} \right) = \frac{\lambda}{4} \left(\frac{\Delta V_{\text{noise}}}{\Delta V_{\text{noise}}} \right). \quad (7)$$

Because the SNR depends on the amplitude of the reference and sensing reflections (5), it is idiosyncratic for each sensor tip and displacement whisker pair. We evaluated the MDD for each pair; if the value was too high, we simply removed a small length of the fiber to create a new sensor tip and rechecked the MDD. We routinely achieved MDD values of 30 nm in air. The MDD increases by about 10% when the sensor is used in isotonic fluid.

D. EFPI Output: An Example

Fig. 4 illustrates the output of the EFPI at each stage of our measurement procedure. The first step is to calibrate the optical fiber sensor [Fig. 4(a)]. The sensor tip is oriented parallel to the reflective displacement whisker and stepped by its attached piezoelectric device (Burleigh Instruments, Inc., Fisher, NY). The magnitude of this step is not important so long as it is greater than 650 nm. In this example, the trace starts at the beginning of a voltage cycle (arrow 1), moves through 35 mV before reversing direction (arrow 2), and then through another 35 mV (to arrow 3) before being swamped by low frequency mechanical vibrations that were excited by the sensor movement. Thus, 35 mV (the peak-to-peak voltage) corresponds to 325 nm of movement.

Following calibration, we measure two displacements [Fig. 4(b)]: 1) displacement of the whisker tip that is in contact with the bundle (top trace) and 2) displacement of the whisker base that is attached to a pipette (bottom trace). First we set a gap distance between the fiber sensor and the reflective displacement whisker such that the output trace begins in the linear range of a voltage cycle [i.e., between the two extremes of interference; Fig. 3(b)]. Then we step the pipette. The top trace shows the signal from the reflective whisker tip. It moves through 28.4 mV (from arrow 1 to arrow 2), which can be converted to a displacement using linear proportionality

$$\delta = (325 \cdot \text{nm}) \left(\frac{28.4 \cdot \text{mV}}{35 \cdot \text{mV}} \right) = 264 \cdot \text{nm}. \quad (8)$$

Thus, the whisker tip/ciliary bundle complex moved 264 nm.

The lower trace shows the signal from the whisker base. It completes one cycle (from arrow 1 to arrow 2) plus 10 mV (to arrow 3). One complete cycle corresponds to 650 nm of displacement and the additional displacement is calculated from linear interpolation of the 10-mV signal

$$\delta = 650 \cdot \text{nm} + (325 \cdot \text{nm}) \left(\frac{10 \cdot \text{mV}}{28.5 \cdot \text{mV}} \right) = 764 \cdot \text{nm}. \quad (9)$$

Thus, the pipette/whisker base complex moved 764 nm.

We can calculate bundle stiffness from these displacements using (4)

$$k_B = k_W \left(\frac{\Delta x_P}{\Delta x_B} - 1 \right) = k_W \left(\frac{764 \cdot \text{nm}}{264 \cdot \text{nm}} - 1 \right) = 1.894 k_W. \quad (10)$$

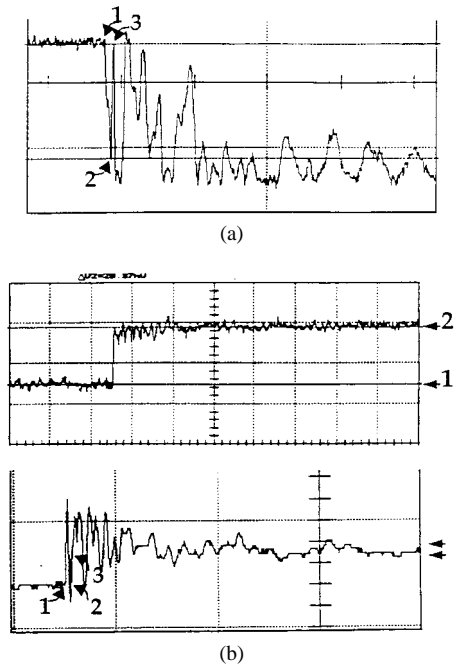


Fig. 4. Measuring bundle displacement with the EFPI. An example: (a) *calibrating the sensor*. The sensor is oriented normal to the reflective displacement whisker and stepped through a distance greater than 650 nm. The resulting peak-to-peak voltage represents 325 nm. In this example, the trace starts from the top of a voltage cycle (arrow 1) and goes through a 35 mV change (arrow 2) before it reverses direction (scale = 20 mV/div). Thus, 35 mV = 325 nm of movement. One voltage cycle (650 nm) is complete at arrow 3. (b) *Measuring displacements*. Two displacement measurements are required to calculate bundle stiffness: 1) displacement of the whisker tip, which is in contact with the bundle (Δx_B), and 2) displacement of the whisker base, which is held in the pipette (Δx_P). (top) Bundle displacement (Δx_B). The sensor for one EFPI channel is positioned by its piezo stepper so that it is normal to the displacement whisker tip and in the linear range of its cosine interference curve [Fig. 2(b)]. Then the whisker is stepped. In the example, the resulting voltage change is 28.4 mV (arrow 1 to arrow 2). This can be converted to a displacement using linear proportionality. Thus, the whisker tip/bundle is displaced 264 nm. $\Delta x_B = (325 \text{ nm}) * (28.4 \text{ mV}/35 \text{ mV}) = 264 \text{ nm}$. (bottom) Pipette displacement (Δx_P). The sensor for the second EFPI channel measures the displacement of the pipette-whisker base. Because the pipette is always stepped through more than 650 nm, it provides the calibration for its own EFPI channel. In the example, the signal goes through one complete voltage cycle (650 nm; arrow 1 to arrow 2) and part of a second cycle (to arrow 3). The peak-to-peak voltage of the first voltage cycle is 28.5 mV; thus, 28.5 mV = 325 nm. The partial voltage cycle (arrow 2 to arrow 3) represents 6 mV (20 mV per division). Thus, the pipette is displaced 718 nm: $\Delta x_P = 650 \text{ nm} + (325 \text{ nm} * (6 \text{ mV}/28.5 \text{ mV})) = 718 \text{ nm}$. We identify the end of the signal in two ways: a) the major frequency decreases suddenly and b) when the mechanical vibration stops (double arrows at right) the final voltage corresponds to the voltage at which the signal stops (arrow 3). This end voltage is determined more readily when the sweep speed is reduced (B, top, above; Fig. 6) At arrow 3 the signal is swamped by an oscillation that represents mechanical (nonaxial) vibration excited by the sensor movement. This occurs frequently (Fig. 6), but it does not compromise our ability to read displacements <325 nm (i.e., bundle displacements) because these are simply the difference between stable start and final voltages (B, top, above; Fig. 6).

The stiffness of the displacement whisker in this example was $k_W = 2.15 \cdot 10^{-4} \cdot \text{N/m}$, which gives a bundle stiffness of $k_B = 4.07 \cdot 10^{-4} \cdot \text{N/m}$.

III. RESULTS

A. Imitation Ciliary Bundles

We tested the performance of the EFPI by using it to measure displacements of imitation ciliary bundles whose

TABLE I

RESULTS OF FIVE EXPERIMENTS TO VALIDATE OUTPUT OF THE EFPI. COLUMN 2 SHOWS THE STIFFNESS OF THREE IMITATION CILIARY BUNDLES MEASURED WITH STYRENE BEADS. COLUMN 3 SHOWS THE STIFFNESS OF THESE SAME IMITATION BUNDLES WHEN MEASURED WITH THE EFPI; BUNDLES II AND III WERE ASSESSED IN AIR AND IN WATER. COLUMN 4 SHOWS THAT RESULTS FROM BOTH METHODS ARE VERY SIMILAR. THE ERROR IS EXPRESSED AS A PERCENTAGE OF THE MEAN BEAD STIFFNESS (ERROR = DIFFERENCE BETWEEN MEASUREMENTS/MEAN BEAD STIFFNESS)

Imitation Bundle	Mean Bead Stiffness	Mean EFPI Stiffness	Error between Averages
	Avg. \pm Std. Dev. (N) $\times 10^{-4}$ N/m		
Bundle I - air	4.03 \pm 0.39 (5)	3.74 \pm 0.54 (12)	7.2
Bundle II - air	3.08 \pm 0.22 (11)	2.90 \pm 0.62 (10)	5.5
Bundle II - water	-----	3.02 \pm 0.31 (14)	1.9
Bundle III - air	3.12 \pm 0.13 (6)	2.92 \pm 0.23 (11)	6.4
Bundle III - water	-----	3.01 \pm 0.20 (14)	3.7

stiffnesses had been determined previously. The imitation bundles were fine glass whiskers fabricated as described for displacement whiskers (see Equipment and Methods) except that they had stiffnesses in the range of those reported for living ciliary bundles [7]. We mounted each imitation bundle on a pipette, measured its stiffness in 5–11 trials using styrene beads of different sizes, and averaged these measurements to get an “average bead stiffness” (Table I, column 2).

We then measured the stiffness of the same imitation bundle with the EFPI. We positioned the imitation bundle so that it could be viewed axially using light microscope optics (Fig. 3) and determined its stiffness using the EFPI and the experimental protocol described above (see Equipment and Methods). We made such EFPI measurements on three imitation bundles: we tested two of these in air and while the “bundle” was submerged in the Ringer’s solution used to maintain living ciliary bundles. In the latter experiments, we attempted to duplicate procedures used on living bundles as closely as possible. A third imitation bundle was tested in air only. Thus, we conducted five experiments to validate the EFPI (Table I, columns 1 and 3).

Experiments involved 10–14 trials, each yielding two displacement measurements (Δx_B , Δx_P). We examined these data in two ways. First, we calculated a stiffness for each trial using (4) and the previously measured stiffness of the deflection whisker ($k_W = 2.15 \pm 0.08 \times 10^{-4}$ N/m). We averaged these stiffness values to get a “mean EFPI stiffness” for the imitation bundle (Table I, column 3). Then, we calculated a percent error between the bead and EFPI stiffness values; this error averaged 4.9% (range 1.9%–7.2%; Table I, column 4).

We examined the data in a second way by plotting the results from each trial as force (F) versus deflection (Δx_B) where

$$F = k_W \Delta x_W = k_W (\Delta x_P - \Delta x_B). \quad (11)$$

Results from one experiment are shown in Fig. 5. The triangles represent the force (F) versus deflection (Δx_B) results for each trial. The solid line is the mean EFPI stiffness for that imitation bundle (bundle II, in water). For comparison, the dashed line shows the stiffness of the same imitation bundle when measured with the styrene bead technique (Table I, col-

umn 2). The difference between the two methods of stiffness measurement is 1.9%. Table I summarizes results for all five experiments.

B. Living Ciliary Bundles

In addition to testing the EFPI on imitation ciliary bundles, we measured the stiffness of living ciliary bundles from the posterior semicircular canal of red-eared turtles, *Pseudemys (Trachemys) scripta*. We anesthetized turtles with Nembutal (2 ml/kg), perfused them with oxygenated turtle Ringer’s solution [15], removed the membranous labyrinth, exposed the posterior crista (the hair cell-bearing region of the posterior semicircular canal), positioned it in a temperature-controlled bath of turtle Ringer’s solution, and viewed the ciliary bundles axially using a Zeiss Axioplan microscope equipped with a 40 \times water-immersion objective (N.A. 0.75; working distance 1.9 mm) and DIC optics. We selected bundles for measurement that appeared intact and relatively isolated to help insure that the displacement whisker did not come in contact with additional bundles. We followed the guidelines of the Ohio University Animal Care and Use Committee in all experiments.

Results from two experiments are shown in Fig. 6. For one bundle [Fig. 6(a)], the signal amplitude is 26 mV, which corresponds to a displacement of 219 nm and a stiffness of 8.7×10^{-4} N/m. For the second bundle [Fig. 6(b)], the signal is 30 mV, which corresponds to a displacement of 263 nm and a stiffness of 6.8×10^{-4} N/m. Both stiffness values are within the range of measured values for vertebrate hair cells [7].

To insure that the signal we measured derived from the displacement whisker only (not from stray reflections off adjacent regions of the target bundle or off neighboring bundles), we determined that living ciliary bundles do not reflect enough light to be detected with our instrument. We did this in two ways. With the sensor tip positioned normal to a ciliary bundle we verified that there was no change in the output signal when 1) we stepped the sensor (as if for a calibration measurement) or 2) we deflected the bundle using a displacement whisker applied to the opposite side of the bundle and so hidden from the sensor by the bundle itself.

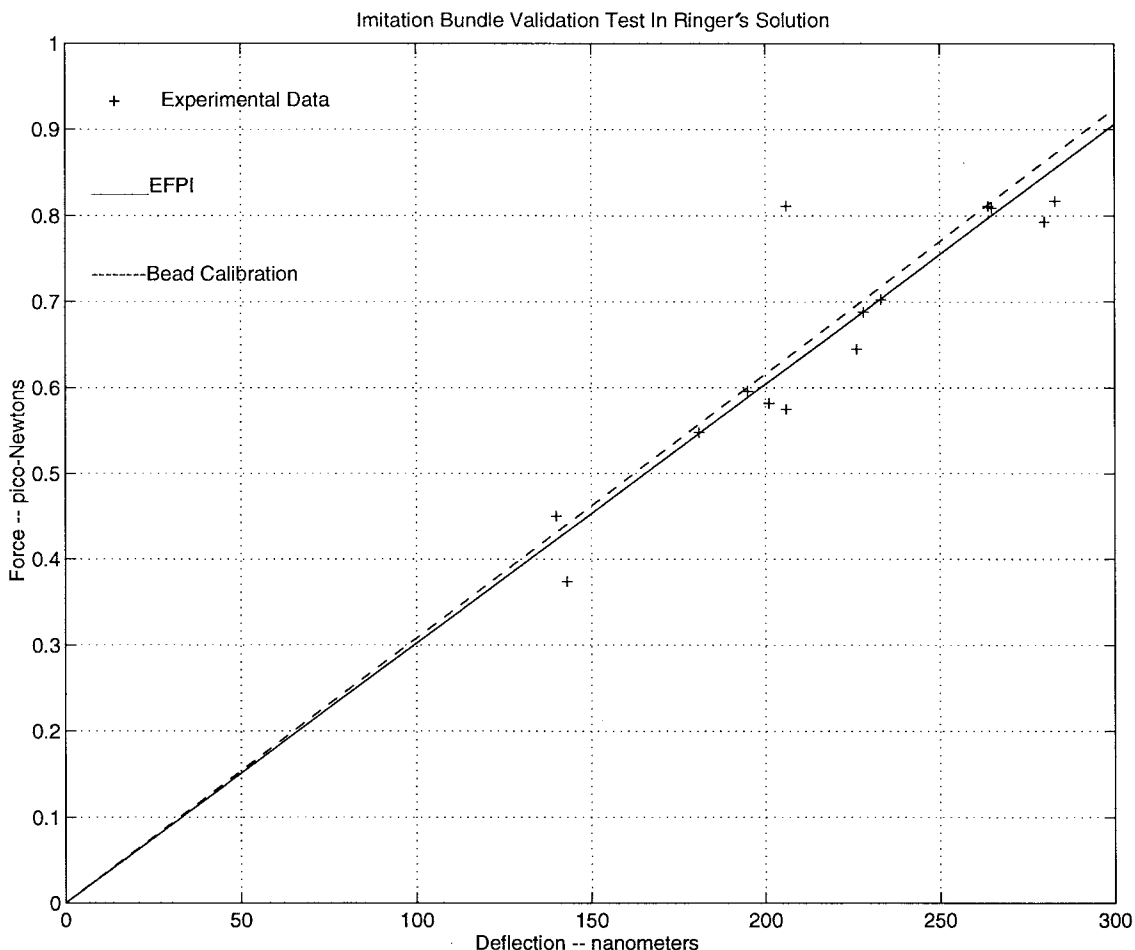


Fig. 5. Testing the EFPI on imitation ciliary bundles of known stiffness. Data points are force versus deflection results for imitation bundle II in fluid (Ringer's solution), as measured by the EFPI. The solid line is the average slope for all data points ("mean EFPI stiffness": 3.02×10^{-4} N/m) with the y -intercept forced through zero (zero force, zero displacement). The dashed line is similarly constructed using the average slope of the bead weight calibrations ("mean bead stiffness": 3.08×10^{-4} N/m) for the same bundle (see Table I). This was a best agreement between the bead and EFPI measurements of stiffness, with an error of 1.9%. Note that deflection magnitudes with the two methods differed by approximately two orders of magnitude, with the bead method being the larger (see Section IV).

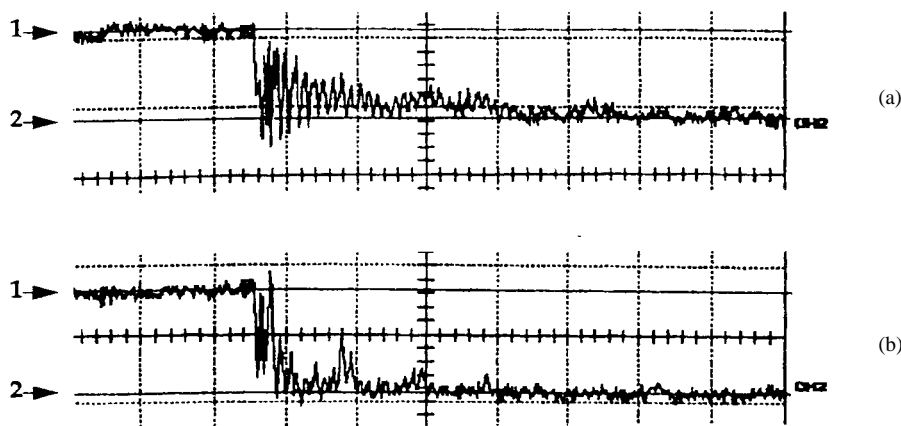


Fig. 6. Voltage output during displacement of living ciliary bundles. Two examples are illustrated from hair cells in the posterior semicircular canal. Our bundle displacements are always less than 325 nm [see Fig. 4(b)]; thus, Δx_B (bundle displacement) is proportional to the difference between starting (arrow 1) and ending (arrow 2) voltages [see Fig. 4(b), top]. Both stiffness values are within the range of measured values for vertebrate hair cells [7]. Because these bundles are close in proximity, we cannot exclude the possibility that in one or both cases the displacement whisker contacted more than one bundle, so single canal bundles may be less stiff than these numbers suggest: (a) the voltage change is 26 mV (20 mV per division), which corresponds to a displacement of 219 nm and a stiffness of 8.7×10^{-4} N/m and (b) the voltage change is 30 mV, which corresponds to a displacement of 263 nm and a stiffness of 6.8×10^{-4} N/m. The voltage-displacement relation is different in (a) and (b) because this relation is established empirically for each experiment.

IV. DISCUSSION

We have developed an improved method for measuring the stiffness of living ciliary bundles on hair cells of the inner ear. Our method relies on a two-channel EFPI that uses fiberoptic sensors to measure: 1) the stimulus delivered to the ciliary bundle and 2) the bundle's response. We verified the accuracy of our method by testing imitation ciliary bundles of known stiffness. In addition, we measured the stiffness of living ciliary bundles in the posterior semicircular canal and obtained values similar to those in the published literature.

A. Advantages of the Two-Channel EFPI

Our instrumentation and measurement protocol have several advantages over previous methods of measuring ciliary bundle stiffness. First, interferometers—especially multiple beam interferometers like the EFPI—provide extremely accurate measurements of small displacements. Thus, they are well suited for measuring physiological deflections of ciliary bundles and distinguishing small stiffness differences between heterogeneous bundle types.

Second, the extrinsic cavity and fiberoptic delivery system of the EFPI allows us to direct the fine sensor tip at any bundle on the neuroepithelium while visualizing the bundle-sensor complex using high power microscope objectives. Thus, we can assess bundles *in situ*, and avoid the mechanical disruption of delicate bundle components that may accompany hair cell dissociation or stripping the neuroepithelium away from its connective tissue base.

Third, the accuracy of our measurements is further enhanced by our calibration procedure. For displacements greater than 325 nm, the calibration value (peak-to-peak voltage produced by a 325-nm displacement) can be read directly from the measurement trace; thus, calibration is inherent in the measurement. For smaller displacements, we calibrate the system immediately before each measurement instead of at the beginning and end of a measurement series. This reduces the danger that changing experimental conditions will lead to measurement errors or force rejection of a measurement series if the calibration values change.

Finally, we measure both the step applied to the bundle and the bundle's deflection with the EFPI, and we use the ratio of these displacements to calculate bundle stiffness. Thus, we need not rely on the accuracy of the stepper's stated output, and the ratio removes any constant error in our measurements. Furthermore, the error we see in measuring one movement with both EFPI channels (3% in our current instrument) tells us the minimum stiffness difference between bundles that we can reliably detect.

B. Sources of Error

The greatest source of error in our measurements is probably the manufacture and calibration of the displacement whiskers. One potential problem is the adhesive used to attach the displacement whisker to the pipette; however, the adhesive we used was sufficiently stiff that we detected no creep under the minute weights of the styrene beads. A greater problem is that our accuracy in measuring bead diameters

and deflections when assessing stiffness of the displacement whiskers is limited by the optics of the microforge scope which had a maximum magnification 200 \times .

Finally, the range of deflections and forces (weights) used to calibrate the displacement whisker are larger than the nanometer deflections and picoNewton forces we use during stiffness measurements with the EFPI. However, they are sufficiently small that we assume linearity of displacement whisker and imitation bundle stiffness across the range of displacements and forces we used in this work.

C. Limitations and Future Improvements

The threshold sensitivity (MDD) of our current system is approximately 30 nm, which is sufficient to measure physiological displacements of ciliary bundles. Greater sensitivity [decreased (MDD)] should be achievable by decreasing system noise that is present in the instrument; no attempt to do so was undertaken.

A second limitation of our current system is the diameter of the unetched sensor tip of approximately 125 μm , of which 9 μm is the optic fiber core (standard core diameter for 1300-nm light) and 116 μm is the surrounding cladding. Etching reduces the sensor diameter by removing cladding, which increases the light loss of the fiber and reduces signal intensity. So some compromise is necessary. In practice, we etched the sensor tip to a diameter of approximately 33 μm , which is close to the evanescent field. Etching, beyond the 33- μm diameter, resulted in loss of a signal, making displacement measurements difficult or impossible. With the sensor tip near the surface of the neuroepithelium, the resulting light spot is approximately the same diameter as the etched fiber tip, which makes it difficult to assess the shortest bundles. For these hair cells it may be necessary to build a second generation instrument using a smaller optical fiber core or use a signal processing technique. Future signal processing of the reflective signal from the bundles could be beneficial.

A complication with our system is the need for a reflective target. Living bundles do not generate usable reflections without additional signal processing [16]; thus, we use the reflective displacement whisker as our target, which has advantages and disadvantages. Although cleaned glass whiskers appear to stick firmly to the bundles (bundles can be pushed or pulled by attached displacement whiskers), we cannot absolutely exclude the possibility of some movement between bundle and displacement whisker. On the other hand, use of the easily visible displacement whisker means that we know precisely the site on the bundle whose movement we measure with the EFPI.

REFERENCES

- [1] A. C. Crawford and R. Fettiplace, "The mechanical properties of ciliary bundles of turtle cochlear hair cells," *J. Physiol. Lond.*, vol. 364, pp. 359–379, 1985.
- [2] J. Howard and J. F. Ashmore, "Stiffness of sensory hair bundles in the sacculus of the frog," *Hearing Res.*, vol. 23, pp. 93–104, 1986.
- [3] J. Howard and A. J. Hudspeth, "Mechanical relaxation of the hair bundle mediates adaptation in mechano-electrical transduction by the bullfrog's saccular hair cell," *Proc. Nat. Acad. Sci. USA*, vol. 84, pp. 3064–3068, 1987.

- [4] I. J. Russell, G. P. Richardson, and M. Kossl, "The responses of cochlear hair cells to tonic displacements of the sensory hair bundle," *Hearing Res.*, vol. 43, pp. 55–70, 1989.
- [5] D. Strelhoff and A. Flock, "Stiffness of sensory-cell hair bundles in the isolated guinea pig cochlea," *Hearing Res.*, vol. 15, pp. 19–28, 1984.
- [6] J. Brix and G. A. Manley, "Mechanical and electromechanical properties of the stereociliary bundles of isolated and cultured hair cells of the chicken," *Hearing Res.*, vol. 76, pp. 147–157, 1994.
- [7] Y. M. Szymko, P. S. Dimitri, and J. C. Saunders, "Stiffness of hair bundles in chick cochlea," *Hearing Res.*, vol. 59, pp. 241–249, 1992.
- [8] W. Denk, W. W. Webb, and A. J. Hudspeth, "Mechanical properties of sensory hair bundles are reflected in their Brownian motion measured with a laser differential interferometer," *Proc. Nat. Acad. Sci., USA*, vol. 86, pp. 5371–5375, 1989.
- [9] R. K. Duncan, H. N. Hernandez, and J. C. Saunders, "Relative stereocilia motion of chick cochlear hair cells during high-frequency water-jet stimulation," *Auditory Neurosci.*, vol. 1, pp. 321–329, 1995.
- [10] S. S. Pae and J. C. Saunders, "Intra- and extracellular calcium modulates stereocilia stiffness on chick cochlear hair cells," *Proc. Nat. Acad. Sci. USA*, vol. 91, pp. 1153–1157, 1994.
- [11] K. A. Murphy, M. F. Gunther, A. M. Vengsarkar, and R. O. Claus, "Quadrature phase-shifted, extrinsic Fabry–Perot optical fiber," *Opt. Lett.*, vol. 16, pp. 273–275, 1991.
- [12] C. E. Lee and H. F. Taylor, "Interferometric optical fiber sensors using internal mirrors," *Electron. Lett.*, vol. 24, pp. 93–94, 1988.
- [13] J. L. Santos, A. P. Leite, and D. A. Jackson, "Optical fiber sensing with a low-finesse Fabry–Perot cavity," *Appl. Opt.*, vol. 31, pp. 7361–7366, 1992.
- [14] R. O. Claus, M. F. Gunther, A. Wang, and K. A. Murphy, "Extrinsic Fabry–Perot sensor for strain and crack opening displacement measurements from -200° to 900° ," *Smart Materials and Structures*, vol. 1, pp. 237–242, 1992.
- [15] J. Hounsgaard and C. Nicholson, "The isolated turtle brain and the physiology of neuronal circuits," in *Preparations of Vertebrate Central Nervous System in Vitro*, J. H. London, Ed. New York: Wiley, 1990, pp. 155–181.
- [16] F. Willemin, S. M. Khanna, and R. Dandiker, "Heterodyne interferometer for cellular vibration measurement," *Acta Otolaryngol.*, suppl. 467, pp. 35–42, 1989.



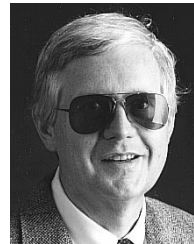
Matthew D. Barrett received the B.S. degree in mechanical engineering in 1994 and the M.S. in engineering mechanics in 1996, from Virginia Polytechnic Institute and State University, Blacksburg.

He is now employed by Michelin Inc., Clermont-Ferrand, France.

Ellengene H. Peterson received the B.A. degree in classics from Radcliffe College, Cambridge, MA, in 1962 and the Ph.D. degree in physiological psychology from the University of California, Riverside, in 1976.

She specialized in neuroanatomy during postdoctoral positions at the University of California, San Diego, and the University of Chicago, Chicago, IL. She is now a Professor in the Department of Biological Sciences and the Neurobiology Program at Ohio University, Athens, where she conducts research on the organization of central vestibular circuits and vestibular hair cells.

Dr. Peterson is a member of the Society for Neuroscience, Association for Research in Otolaryngology, AAAS, and NYAS.



J. Wallace Grant received the B.S. degree in mechanical engineering from West Virginia Institute of Technology, Montgomery, in 1965. He worked in the chemical process industry for several years and then entered graduate school at Tulane University, New Orleans, LA, where he received the M.S. degree in 1970 and the Ph.D. degree in 1973, both in mechanical engineering with a specialty in biomechanics. While at Tulane he also attended medical school.

He was then employed by the DuPont Co., Wilmington, DE, as a Senior Research Engineer in their life sciences division. He joined the Department of Engineering Science and Mechanics at Virginia Polytechnic Institute and State University as an Assistant Professor in 1980. He is now a Professor in the same department. He has published numerous journal articles and made many presentations on the biomechanics of the vestibular system.

Dr. Grant is a member of the Biomedical Engineering Society, Association for Research in Otolaryngology, Aerospace Medical Association, ASME, and ASEE.